

AD-A250 928



ation is estimated to average 1 hour per response, including the time for reviewing instructions, searching existing data sources, completing and reviewing the collection of information. Send comments regarding this burden estimate or any other aspect of this reducing this burden to Washington Headquarters Services, Directorate for Information Operations and Reports, 1215 Jefferson 7, and to the Office of Management and Budget, Paperwork Reduction Project (0704-0188), Washington, DC 20503

2. REPORT DATE  
5/29/923. REPORT TYPE AND DATES COVERED  
Technical

5. FUNDING NUMBERS

R &amp; T Code:

413n008

G N00014-88-K-0483

## 6. AUTHOR(S)

William R. Peifer, M. Todd Coolbaugh,  
and James F. Garvey

## 7. PERFORMING ORGANIZATION NAME(S) AND ADDRESS(ES)

Dept. of Chemistry, Acheson Hall  
State University of New York at Buffalo  
Buffalo, NY  
14214

8. PERFORMING ORGANIZATION  
REPORT NUMBER

Technical Report  
# 24

## 9. SPONSORING/MONITORING AGENCY NAME(S) AND ADDRESS(ES)

Dr. R. DeMarco/Dr. J. Pazik, Chemistry Division  
Office of Naval Research  
800 N. Quincy St.  
Arlington, VA  
22217

10. SPONSORING/MONITORING  
AGENCY REPORT NUMBER

## 11. SUPPLEMENTARY NOTES

## 12a. DISTRIBUTION/AVAILABILITY STATEMENT

Approved for public release;  
distribution unlimited

## 12b. DISTRIBUTION CODE

## 13. ABSTRACT (Maximum 200 words)

A review of our gas phase cluster work with potential application  
to the generation of new materials (i.e, cluster assembled thin films)

DTIC  
ELECTE  
JUN 03 1992  
S A D

## 14. SUBJECT TERMS

## 15. NUMBER OF PAGES

## 16. PRICE CODE

17. SECURITY CLASSIFICATION  
OF REPORT  
UNCLASSIFIED

18. SECURITY CLASSIFICATION  
OF THIS PAGE  
UNCLASSIFIED

19. SECURITY CLASSIFICATION  
OF ABSTRACT  
UNCLASSIFIED

20. LIMITATION OF ABSTRACT  
UL

OFFICE OF NAVAL RESEARCH

GRANT N00014-88-K-0483

R & T Code 413n008

Technical Report No. 24

**Chemistry within Molecular Clusters**

by

William R. Peifer, M. Todd Coolbaugh, and James F. Garvey\*

Prepared for Publication  
in

Clusters and Clustering from Atom to Fractals

Edited by P. Reynolds, North-Holland, Amsterdam,

Acheson Hall  
Department of Chemistry  
University at Buffalo  
The State University of New York at Buffalo  
Buffalo, NY  
14214

June 1, 1992

Reproduction in whole or in part is permitted for any purpose of the United States Government

This document has been approved for public release and sale; its distribution is unlimited

**92-14326**



92 6 01 014

# Chemistry within Molecular Clusters

William R. Peifer,  
M. Todd Coolbaugh  
and  
James F. Garvey\*

Acheson Hall, Department of Chemistry  
State University of New York at Buffalo  
Buffalo, NY 14214

## 1 Introduction

The physics of weakly bound van der Waals has been studied recently is a variety of ways to gain an understanding of their formation and to determine their various physical properties. However, the study of chemical reactions within clusters is especially intriguing, since clusters can bridge the disparate field of bimolecular gas-phase reaction dynamics and solution chemistry. By examining the chemistry within these cluster systems it is possible to directly learn how the behavior of the system changes as a function of stepwise solution, thereby leading to an understanding of the factors which govern reactions in solution that are absent in gas phase processes.

Most of the recent work in this area consists of utilizing the neutral cluster as one of the reagents for a bimolecular reaction<sup>1-8</sup>, with the product cluster ion being directly detected via conventional mass spectrometric techniques. Apart from the observation of protonated clusters there are a few reported cases of chemical reactions taking place within the cluster ion itself.<sup>9-22</sup> In addition to this typical unimolecular and bimolecu-



Availability Codes	
Dist	Avail and/or Special
A-1	

lar gas-phase chemistry already studied within clusters, we have recently observed the generation of new cluster product ions which cannot be explained by either of these two known processes. The new processes have absolutely no counterpart in gas-phase bimolecular reactions, and only occur within van der Waals clusters.<sup>23</sup> They include the generation of  $(C_2H_4F_2)_{n \geq 4}H^+$  ions from 1,1-difluoroethane clusters,<sup>24</sup> the generation of  $(CH_3OCH_3)_nH_3O^+$  and  $(CH_3OCH_3)_nCH_3OH^+$  ions from dimethyl ether clusters,<sup>25,26</sup> the generation of  $(NH_3)_nN_2H_5^+$  ions from ammonia clusters<sup>27</sup> and the photogeneration of  $MoO^+$  and  $MoO_2^+$  ions from van der Waals clusters of molybdenum hexacarbonyls.<sup>28</sup> The observation of these new chemical processes which occur only within a cluster means that one may now utilize clusters as a novel "crock-pot" in which to produce new molecules.

Thus, while the study of reactive processes in clusters may be used as a bridge between the gas-phase "bimolecular" and the "solvated multimolecular" world of chemical reactions, we feel that this bridge has in fact turned into a crossroads: new chemical reactions and unexpected dynamics exist which occur only within the condensed environment of a molecular cluster. We will give illustrative examples wherein this new chemistry within clusters occurs through:

1. stabilizing unstable reagents
2. stabilizing unstable intermediates
3. providing new chemical pathways.

## 2 Experimental Method

The majority of our experiments consist of generating a beam of neutral van der Waals clusters, colliding them with electrons and performing mass spectroscopy on the resulting cluster ion species within the beam. Though cations are rapidly generated within the cluster ( $10^{-14}$  s), it takes microseconds before the resulting cluster ion migrates out of the ionizer region and is then mass selected by the quadrupole filter. On this lengthy time scale the solvated cation may rid itself of its excess energy by fragmentation of the cation, by evaporation of neutral monomers from the cluster ion, or by chemically reacting with one (or more!) of the solvating neutrals. In any case, a new product cluster ion is generated, which is then detected via mass spectroscopy.

One may visualize the electron impact ionizer part of our apparatus as a 'reaction cell' in which precursor cluster ions are generated and allowed to 'incubate' for microseconds, and subsequently the newly generated product ions are analyzed via mass spectroscopy. By observing the distribution of product cluster ions in the mass spectra, we deduce the ion-molecule chemistry which is occurring within the bulk cluster, and observe how this chemistry changes as a function of cluster size.

For the metal hexacarbonyl experiments (section 3.3.2) a different beam apparatus is used. Helium, seeded with a metal carbonyl compound at room temperature vapor pressure (typically a few hundred mTorr), is admitted into the low-volume stagnation region of a Newport BV-100 pulsed molecular beam valve fitted with an end plate having a 0.5 mm diameter, 30° conical aperture. Metal hexacarbonyl van der Waals complexes are then formed in the free-jet expansion of the pulsed beam of seeded helium. Operation of the valve at 1 Hz leads to maximum chamber pressures of about  $3 \times 10^{-6}$  torr. The cluster beam pulse is directed axially into the ion source of a Dycor M200M quadrupole mass spectrometer, where it is intersected by the focused output from a Lambda Physik EMG 150 excimer laser, operated on the KrF\* transition at a pulse energy of ca. 100 mJ. Synchronization of the laser and the molecular beam valve is accomplished through the use of an external timing circuit with an adjustable delay.

### 3 Results and Discussion

#### 3.1 Stabilizing an Unstable Reagent within the Solvating Confines of a Cluster

The dominant reactive process which occurs within our cluster ions ( $M_{n-1}M^+$ , where M is the monomeric unit) consists of a bimolecular reaction between the monomer cation and one of the neutral solvent molecules. This generates a protonated cluster ion and a radical. Such a 'protonation' reaction has been well studied in a variety of bimolecular gas phase experiments and is observed to occur for a wide range of molecules. In many cases these reactions are highly exoergic and quite facile. Therefore, a molecular cluster

mass spectrum is usually dominated by the appearance of cluster ions with the empirical formula  $M_nH^+$ .

However, for many organic molecules, upon electron impact ionization the parent ion is unstable. That is, the ground state cation ( $M^+$ ) is thermodynamically unstable with respect to fragmentation. In such cases the mass spectrum is composed solely of fragment ions, and identification of the molecule must be made by the characteristic fragmentation pattern.

The mass spectrum of 1,1-difluoroethane (DFE) represents just such a case. Since the parent ion is unstable, we expect that the protonation reaction



will not occur within the  $(C_2H_4F_2)_n$  cluster, since the parent ion never survives long enough to react with one of the solvating monomers. Hence, the cluster mass spectrum of DFE should have a complete absence of peaks with the formula  $M_{n-1}H^+$ , and be composed solely of solvated fragment ions. Figure 1 shows a EI (electron impact) mass spectrum of DFE clusters as a function of cluster size and product channel i.e., channel 1:  $M_{n-1}CH_3CFH^+$ , channel 2:  $M_{n-1}C_2H_3F^+$ , channel 3:  $M_{n-1}C_2H_3F_2^+$ , and channel 4  $M_{n-1}H^+$ . We note that in addition to the expected fragmentation (channels 1-3) another sequence of peaks which have the empirical formula of  $M_{n-1}H^+$  appear at  $n = 4$  and continues to become progressively more prominent with increasing cluster size. This is in direct contrast to the fragment channels which monotonically decrease with increasing cluster size and contradicts the expected absence of  $M_nH^+$  in light of the instability of the precursor ion ( $C_2H_4F_2^+$ ).

This spectrum can be explained<sup>30</sup> if the parent ion is metastable as a result of being formed in the Franck-Condon region of the neutral molecule. That is, if the parent ion is generated within the cluster, the presence of solvating molecules may stabilize it long enough, such that it can react with one of the neutral monomers by reaction 1. The fact that the protonated cluster ions only appear for  $n > 4$ , suggests that  $M_5^+$  is the critical size for stabilizing the monomer ion, in the absence of any monomer evaporation. Any evaporation which might occur, will not affect the qualitative conclusions drawn from this analysis namely that an unstable reagent cation can be stabilized within a cluster long enough that it can undergo reactions with the solvating monomers.

### 3.2 Stabilizing an Unstable Intermediate within the Solvating Confines of a Cluster

Figure 2 shows a small section of a typical 70 eV electron impact mass spectrum for dimethyl ether clusters  $(\text{CH}_3\text{OCH}_3)_n$  (for  $n$  between 2 to 3). In addition to the hydronium ion<sup>25</sup> we also observe a protonated methanol ion solvated by 2 dimethyl ether (DME) molecules. This sequence of cluster peaks is observed systematically throughout the entire cluster mass spectrum to the limit of our sensitivity (all the way up to  $n = 28$ ).

It is interesting to note that while the  $\text{CH}_3^+$  and  $\text{CH}_3\text{OCH}_2^+$  fragment cations are extremely intense in the monomer mass spectrum of DME (54% of all ion intensity), the same cluster cations are substantially reduced in intensity (i.e.,  $(\text{DME})_n\text{CH}_3^+$  and  $(\text{DME})_n\text{CH}_3\text{OCH}_2^+$ ). We speculate that this is due to the fragments being consumed by an ion-molecule reaction within the cluster. A likely candidate is the ion-molecule reaction of the fragment cations with a neutral DME within the bulk cluster, to form a trimethyloxonium cation intermediate. Similar ion-molecule reactions have been previously observed<sup>31</sup>. The newly formed trimethyloxonium cation may then undergo a rearrangement to form the observed products as shown in Figure 2.

This mechanism is similar to that observed for the decomposition of DME over zeolite catalysts. van Hooff, et al.<sup>32</sup> observed that conversion of DME over a zeolite catalyst produced ethylene and propene as primary olefins. To account for their results they invoke a trimethyloxonium intermediate as the common intermediate for the observed products. We therefore speculate that the DME cluster reactions leading to the same products should involve the same mechanism found to occur on zeolite catalysts. That is, within the stabilizing environs of a cluster the trimethyloxonium cation may internally rearrange where it forms protonated methanol (via elimination of ethylene) or protonated water (via elimination of propene).

An analogous process has previously been reported for the collisional activation of the monomer  $(\text{CH}_3)_3\text{O}^+$  ion.<sup>33</sup> However recent additional work appears to be at variance with that original result.<sup>34</sup> We feel this is due to the thermodynamic instability of the bare  $(\text{CH}_3)_3\text{O}^+$  for which unimolecular dissociation can effectively compete with the rearrangement reaction and thus only simple methyl loss is observed. However, within the solvating environs of a cluster (or a zeolite surface) the unstable intermediate may be stabilized on a sufficiently long time scale for the rearrangement reaction to occur.

### 3.3 Providing New Chemical Pathways

#### 3.3.1 Ammonia Clusters<sup>27</sup>

The widely studied ammonia cluster mass spectrum<sup>10,11</sup> is dominated by a sequence of peaks with the empirical formula  $(\text{NH}_3)_n\text{NH}_3^+$  and  $(\text{NH}_3)_n\text{NH}_4^+$ , both corresponding to the already discussed protonation reaction. Careful study of the mass spectrum also reveals another series of peaks which at first glance, appears to have the empirical formula  $(\text{NH}_3)_{n-1}\text{NH}_2^+$ . These latter peaks result from the process of the fragmentation of an N-H bond in the  $\text{NH}_3^+$  cation.

A plot of the relative intensities of the  $(\text{NH}_3)_{n-1}\text{NH}_2^+$  ions as a function of cluster size ( $n$ ) is shown in Figure 3 for a variety of electron energies and nozzle temperatures. A magic number, corresponding to an enhancement in the ion signal, is clearly observed for the cluster ion of size  $n = 7$ . This result is independent of electron energy or cluster expansion conditions. We therefore feel that this intensity distribution is due solely to the stability of the  $(\text{NH}_3)_6\text{NH}_2^+$  cluster ion.

This is at first a very surprising result since magic numbers usually result from the closing of the first solvent shell around the central cation. If the central cation in this case is indeed  $\text{NH}_2^+$ , why does the first solvent shell closure need 6 ammonia? Why wouldn't 2 or 3 solvent molecules suffice?

We can account for the observed size dependence of the  $(\text{NH}_3)_{n-1}\text{NH}_2^+$  cluster ion yield if we assume that an associative ion-molecule reaction occurs between the nascent  $\text{NH}_2^+$  ion and an adjacent  $\text{NH}_3$  solvent molecule within the cluster via the reaction:



From available thermochemical data, we estimate that this reaction is exothermic by 4.52 eV. While the "naked" (unclustered) product of the highly exothermic associative reaction (2) would have sufficient internal energy to undergo subsequent N-H bond cleavage, it would certainly be stabilized through solvation by additional  $\text{NH}_3$  molecules. In fact, if we hydrogen-bond five  $\text{NH}_3$  solvent molecules to the five H atoms of the  $\text{N}_2\text{H}_5^+$



product ion, we end up with an ion having a completed solvation shell with the anticipated empirical formula. The  $(\text{NH}_3)_5\text{N}_2\text{H}_5^+$  structure is illustrated in Figure 4. This cluster ion has a total of seven nitrogen atoms and accounts for our observation of a magic number;  $n = 7$ . It is expected that the exothermicity of reaction (2) should enhance the magic number effect, since this excess heat will serve to "boil off" the loosely bound solvent molecules which are not in the first solvent shell. This is an interesting example, wherein the observation of magic numbers was necessary to elucidate the true chemical identity of the central cation.

### 3.3.2 Metal Hexacarbonyl Clusters

van der Waals clusters of  $\text{M}(\text{CO})_6$  ( $\text{M} = \text{Mo}, \text{W}$ ) generated in the free jet expansion of a pulsed beam of seeded helium are subjected to multiphoton ionization (MPI) and the product ions analyzed by quadrupole mass spectrometry. These species are of fundamental significance to our understanding of metal-metal and metal-ligand bonding interactions, and can serve as model systems for the study of catalysis and surface phenomena. Studies of the effects of cluster size and structure on reactivity of transition metal carbonyl clusters can provide the necessary data with which to test and refine our theories concerning the chemistry and physics of bulk metals.

The multiphoton dissociation and ionization dynamics of mononuclear and covalently bound multinuclear transition metal carbonyls is well characterized: initial multiphoton dissociation (MPD) of the metal carbonyl results in complete ligand stripping, leaving behind a naked metal atom which is subsequently photoionized. Consequently the 248 nm MPI mass spectrum for the  $\text{M}(\text{CO})_6$  monomer is dominated almost exclusively by the  $\text{M}^+$  cation signal.

On the other hand, multiphoton photophysics of van der Waals complexes of transition metal carbonyls is not so thoroughly characterized. Indeed, for MPI of  $\text{M}(\text{CO})_6$  clusters, we observe not only the production of  $\text{M}^+$  but also the oxide ions  $\text{MO}^+$  and  $\text{MO}_2^+$ . Observing the production of these ions as a function of laser intensity reveals that the yield of  $\text{M}^+$  depends on the square root of laser intensity, while the yields for both of the oxide ions are nearly independent of laser intensity (6-210 mJ). This strongly suggests we are observing two distinct processes. The first is a multiphoton dissociation within the cluster leading to a bare metal atom which is subsequently ionized via MPI, generating

the  $M_+$  ion signal. The second process is a photochemically induced intracuster reaction leading to oxomolybdenum ions.

We propose that a novel binuclear adduct arises through an intracuster reaction and that the oxide ions arise by subsequent photoionization and fragmentation of that adduct. That is, within the cluster the photogenerated metal atom can associate with the ligands of an adjacent metal carbonyl "solvent" molecule. We therefore propose, on the basis of orbital symmetry considerations, that the nascent metal "photoatom" interacts with a neighboring metal carbonyl "solvent molecules" via two such bridging carbonyls to form a stable six member structure. Through backdonation of metal  $d_{xy}$  electron density to the empty  $\pi^*$  MO's of the carbonyl ligands, the two C-O bonds weaken and break, eventually resulting in the observed oxide ion formation.

However, we find no evidence of such behavior in the  $Cr(CO)_6$  system. Based on these results for the group VI b hexacarbonyls, we suggest that the reactivity within clusters of first-row transition metal atoms is fundamentally different from that of first-row transition metal atoms is fundamentally different from second- or third-row metals, and is determined by the occupancy and relative size of the metal d orbitals. Based on this model we would predict that the intracuster reaction between a photogenerated metal atom and an adjacent  $M(CO)_6$  cluster molecule depends explicitly on the efficient overlap of the relevant molecular orbitals. In the particular case of Cr, the small d orbital on the metal makes for poor overlap with the carbonyl ligands, hence the lack of reactivity. This model, which invokes different modes of CO coordination, may have important implications for the study of catalysis.

## 4 Future Directions

The four examples presented has represented only the beginning in terms of the new chemistry which can be discovered within clusters.<sup>35</sup> New information will be learned from the use of mass selected cluster beams to directly observe the reaction dynamics, and attempts to probe spectroscopically the internal states of the radical product generated initially within the cluster.

Future applications include the use of clusters to generate novel bulk materials in the form of thin films. We have modified the standard Smalley metal cluster source for such

thin film generation<sup>36</sup>. Preliminary experiments have shown that this source is capable of generating a high temperature material within a beam expansion and depositing that material on a cool substrate. We expect that by tailoring the expansion conditions a variety of high quality homogeneous thin films can be produced with obvious industrial applications (superconducting thin films, diamond-like carbon thin films, patterned or multi-layered thin films, etc...).

Finally, we note that our knowledge concerning the generation of new product cluster ions via chemistry within clusters can be used to alter or modify already existing surfaces. That is, the metastable reactive intermediates often generated within the cluster may be ideal for use as selective surface etchants, or even for CVD type deposition onto a substrate. We have recently acquired a triple quadrupole mass spectrometer, which we now intend to use for mass selected cluster chemistry on a variety of surfaces.

## 5 Acknowledgements

This research was supported by the Office of Naval Research which is hereby gratefully acknowledged.

## 6 References

- (1) Whitehead, J. C.; Grice, R. *Faraday Discuss. Chem. Soc.* 1973, 55, 320.
- (2) King, D. L.; Dixon, D. A.; Herschbach, D. R. *J. Am. Chem. Soc.* 1974, 96, 3328.
- (3) Gonzalez Urena, A.; Bernstein, R. B.; Phillips, G. R. *J. Chem. Phys.* 1975, 62, 1818.
- (4) Behrens, R. B., Jr.; Freedman, A.; Herm, R. R.; Parr, T. P. *J. Chem. Phys.* 1975, 63, 4622.
- (5) Wren, D. J.; Menzinger, M. *Chem. Phys.* 1982, 66, 85.
- (6) Nieman, J.; Na'aman, R. *Chem. Phys.*, 1984, 90, 407.
- (7) Morse, M. D.; Smalley, R. E. *Ber. Bunsenges. Phys. Chem.* 1984, 88, 208.
- (8) Whetten, R. L.; Cox, D. M.; Trevor, D. J.; Kaldor, A. *Surf. Sci.* 1985, 156, 8.
- (9) Hermann, V.; Kay, B. D.; Castleman, A. W., Jr.; *Chem. Phys.* 1982, 72, 185.
- (10) Stephan, K.; Futrell, J. H.; Peterson, K. I.; Castleman, A. W., Jr.; Wagner, H. E.; Djuric, N.; Mark, T. D. *Int. J. Mass Spectrom. Ion Phys.* 1962, 44, 167.
- (11) Echt, O.; Morgan, S.; Dao, P. D.; Stanley, R. J.; Castleman, A. W.; Jr. *Ber. Bunsenges, Phys. Chem.* 1984, 88, 217.
- (12) Stace, A. J.; Shukla, A. K. *J. Phys. Chem.* 1982, 86, 865.
- (13) Grimsrud, E. P.; Kebarle, P. J. *Amer. Chem. Soc.* 1973, 95, 7939. Morgan, S.; Castleman, A. W., Jr. *J. Phys. Chem.* 1989, 93, 4544. *Ibid.*, *J. Am. Chem. Soc.*, 1987, 109, 2868.
- (14) Stace, A. J.; Shukla, A. K. *J. Am. Chem. Soc.* 1982, 82, 5314.
- (15) Stace, A. J.; Moore, C. J. *Am. Chem. Soc.* 1982, 82, 5314.
- (16) Kenny, J. E.; Brumbaugh, D. V.; Levy, D. H. *J. Chem. Phys.* 1979, 71, 4757.
- (17) Klots, C. E.; Compton, R. N. *J. Chem. Phys.* 1978, 69, 1644, Klots, C. E. *Radiat. Phys. Chem.* 1982, 20, 51, *Ibid. Kinetics of Ion-Molecule Reactions*; Ausloos, P., Ed.; Plenum, New York, 1979; p. 69.
- (18) Ono, Y.; Ng, C. Y. *J. Am. Chem. Soc.* 1982, 104, 4752.
- (19) Nishi, N.; Yamamoto, K.; Shinohara, H.; Nagashima, U.; Okuyama, T. *Chem. Phys. Lett.* 1985, 122, 599.
- (20) Stace, A. J. *J. Am. Chem. Soc.* 1985, 107, 755.
- (21) Milne, T. A.; Beachley, J. E.; Greene, F. T. *J. Chem. Phys.* 1972, 56, 3007.
- (22) Ceyer, S. T.; Tiedemann, P. W.; Ng, C. Y.; Mahan, B. H.; Lee, Y. T. *J. Chem. Phys.*

1979, 70, 2138.

(23) Garvey, J. F.; Bernstein, R. B. *Chem. Phys. Lett.* 1986, 126, 394, Garvey, J. F.; Bernstein, R. B. *J. Phys. Chem.* 1986, 90, 3577.

(24) Coolbaugh, M. T.; Peifer, W. R.; Garvey, J. F. *J. Am. Chem. Soc.* 1987, 109, 1921.

(25) Garvey, J. F.; Bernstein, R. B. *J. Am. Chem. Soc.* 1987, 109, 1921.

(26) Coolbaugh, M. T.; Peifer, W. R.; Garvey, J. F. *J. Am. Chem. Soc.* 1990, 112, 3692.

(27) Peifer, W. R.; Coolbaugh, M. T.; Garvey, J. F. *J. Chem. Phys.* 1989, 91, 6684.

(28) Peifer, W. R.; Garvey, J. F. *J. Phys. Chem.* 1989, 93, 5906. *Ibid.* *Int. J. of Mass Spectrom. Ion. Proc.* 1990, 102, 1.

(29) Campargue, R.; Lebehot, A. 9th Int. Symp. Rarefied Gas Dynamics, Gottingen 1974, 11, 1. Campargue, R. *J. Phys. Chem.* 1984, 88, 4466.

(30) Heinis, T.; Bar, R.; Borlin, K.; Jungen, M. *Chem. Phys.* 1985, 94, 235.

(31) Harrison, A. G.; Young, A. B. *Intern. J. of Mass Spectrom. Ion. Proc.* 1989, 94, 321.

(32) van Hooff, J. H. C.; van der Berg, J. P.; Wolthuizen, J. P.; Volmer, A. *Proc. Int. Zeolite, Conf.*, 6th, 1983, 489.

(33) Sigsby, M. L.; Day, R. J.; Cooks, R. G. *Org. Mass Spectrum*, 1979, 14, 274.

(34) Farcasiu, D.; Pancirov, R. G. *Int. J. of Mass Spectrom. Ion Proc.* 1986, 74, 207.

(35) Rosenstock, H. M.; Draxl, K.; Steiner, B. W.; Herron, J. T. *J. Phys. Chem. Ref. Data* 6, 1977, Suppl. Monograph 1. Meot-Ner, M.; Nelsen, S. F.; Willi, M. R.; Frigo, T. B. *J. Am. Chem. Soc.* 1984, 106, 7384.

(36) Coolbaugh, M. T.; Peifer, W. R.; Garvey, J. F. *Chem. Phys. Lett.* 1989, 156, 19. *Ibid.*, *Chem. Phys. Lett.* 1989, 164, 441. *Ibid.* *Accts. of Chem. Res.* 1991, 24, 48, Peifer, W. R.; Coolbaugh, M. T.; Garvey, J. F. *J. Phys. Chem.* 1989, 93, 4700.

(37) Herron, W. J.; Garvey, J. F. *Mat. Res. Soc. Proc.*, Robert S. Averback, David L. Nelson & J. Bernholc, eds., 1991, 206, 391.

### Figure Captions

Figure 1a) Bar graph representing percent yield of daughter cluster ion as a function of parent cluster size ( $n$ ) and process channel (i.e. channel 1:  $M_{n-1}\text{CH}_3\text{CFH}^+$ , channel 2:  $M_{n-1}\text{C}_2\text{H}_3\text{F}^+$ , channel 3:  $M_{n-1}\text{C}_2\text{H}_3\text{F}_2^+$ , and channel 4:  $M_{n-1}\text{H}^+$  and  $M = \text{C}_2\text{H}_4\text{F}_2$ ) at 30 eV electron impact energy. Note how all three of the fragmentation channels drop as a function of the cluster size while the cluster reaction channel (channel 4) increases with  $n$ . Reprinted with permission from reference 24. Copyright 1987 American Chemical Society.

Figure 1b) same as 1a but at 100 eV electron impact energy. Reprinted with permission from reference 24. Copyright 1987 American Chemical Society.

Figure 2) Proposed reactions scheme for dimethyl ether clusters. At the bottom is a raw mass spectrum of neat dimethyl ether cluster at 70 eV from 80 to 140 amu. Major ion peaks are identified by their empirical formulas ( $M = (\text{CH}_3)_2\text{O}$ ). Reprinted with permission from reference 26. Copyright 1990 American Chemical Society.

Figure 3) top panel: A plot of the intensities of the  $(\text{NH}_3)_{n-1}\text{NH}_2^+$  cluster ions vs. cluster size  $n$ . The stagnation pressure was held at 273K during the collection of all mass spectra represented here. Bottom panel: A plot of the intensities of the  $(\text{NH}_3)_{n-1}\text{NH}_2^+$  cluster ions vs. cluster size  $n$ . The mass spectra represented here were all collected at an electron impact energy of 70 eV. Reprinted with permission from reference 27. Copyright 1989 American Institute of Physics.

Figure 4) Proposed structure for the  $(\text{NH}_3)_5\text{NH}_2^+$  cluster ion. This species is the most prevalent of all cluster ions in the series  $(\text{NH}_3)_{n-1}\text{NH}_2^+$ , and is believed to be a protonated hydrazine molecule (within the circle) surrounded by one complete solvation shell of ammonia molecules. The shaded circles correspond to nitrogen atoms while the open circles are hydrogen atoms and the dashed lines indicate hydrogen bonds of the  $\text{NH}_3$  solvent molecules to the  $\text{N}_2\text{H}_5^+$  cation. Reprinted with permission from reference 27. Copyright 1989 American Institute of Physics.

a) 30 eV

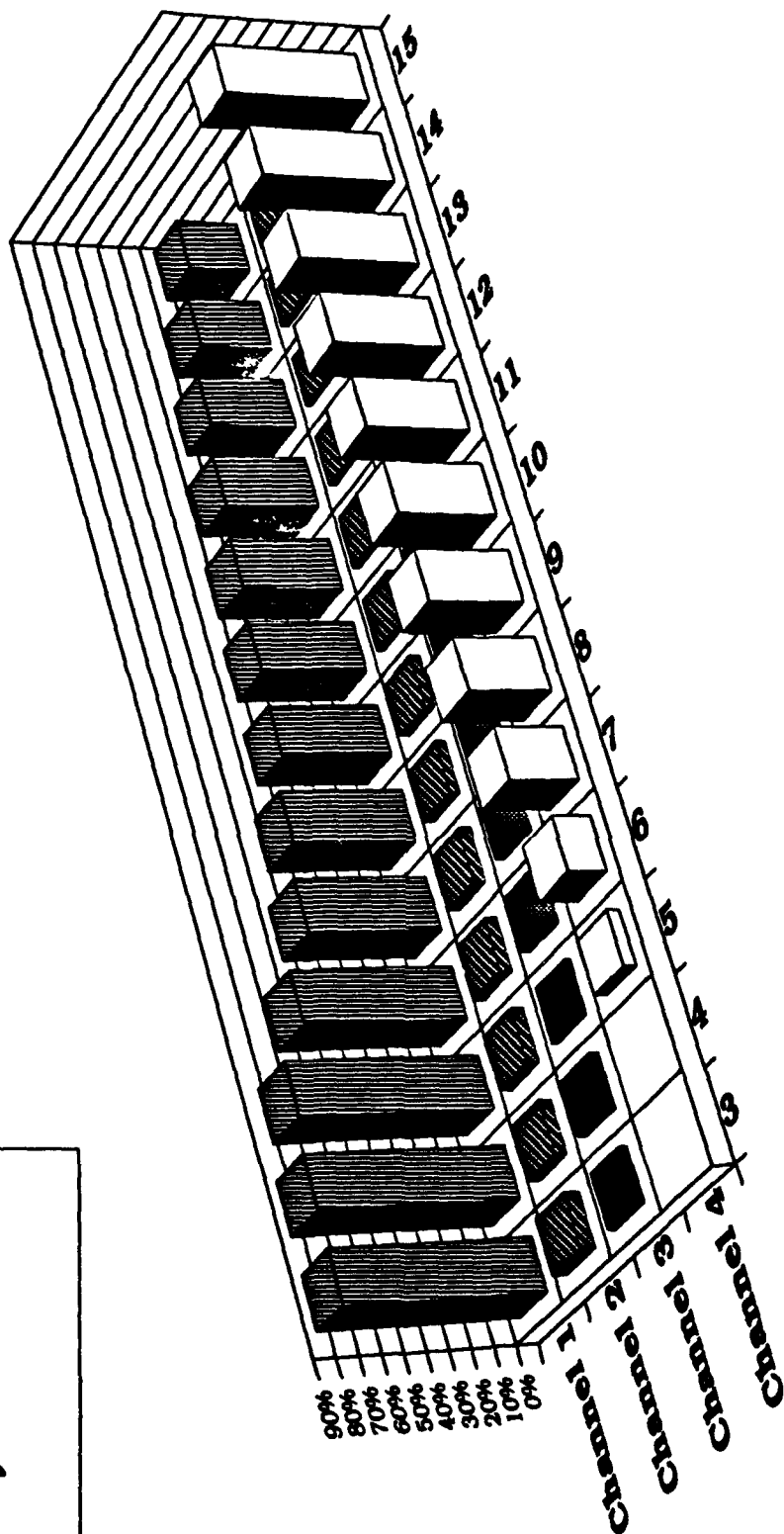


FIGURE 1A 'CUMULATIVE' DATA: PERCENTAGE OF CHANNELS 1-16

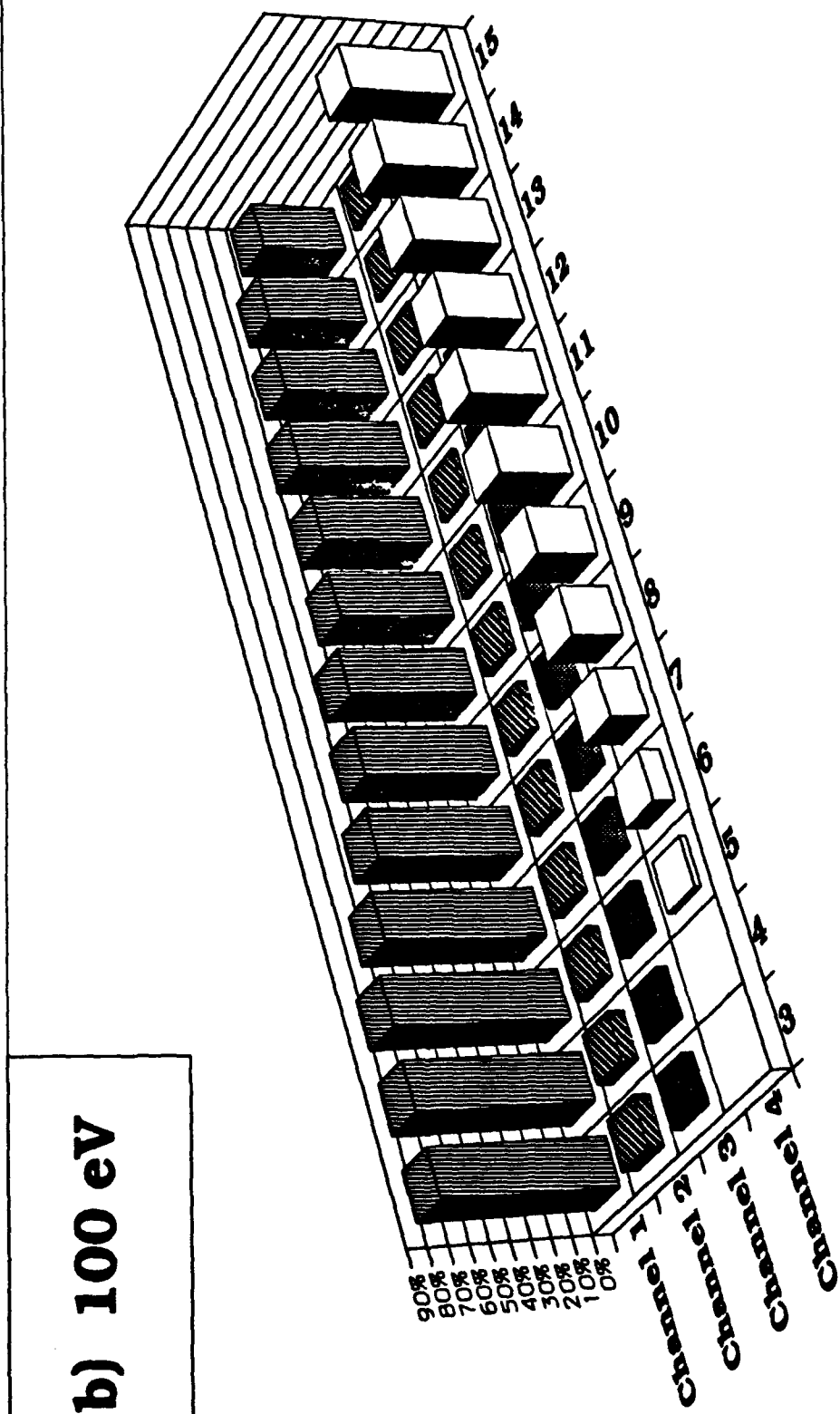
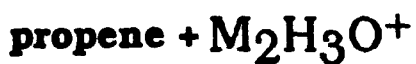
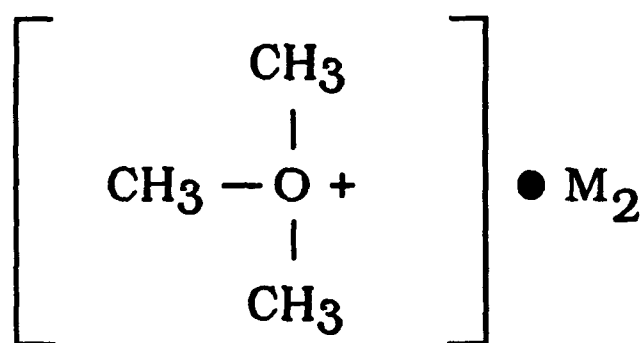
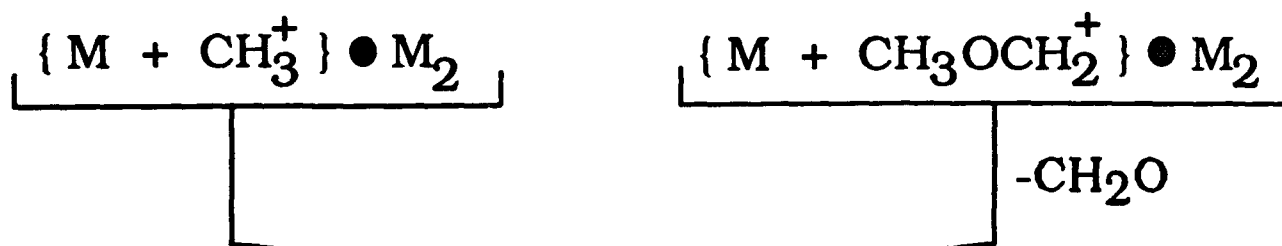
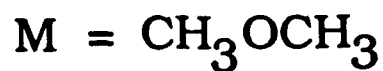


Figure 1b: (continued) with a different crystal before





Ion Intensity (arb. units)

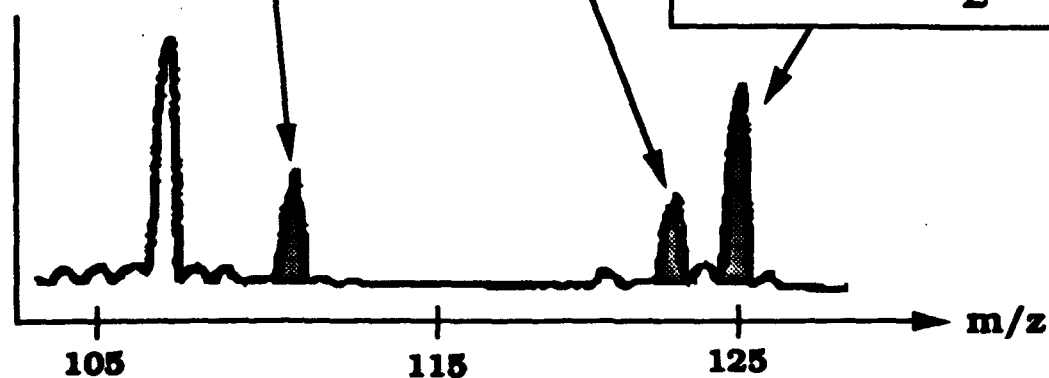
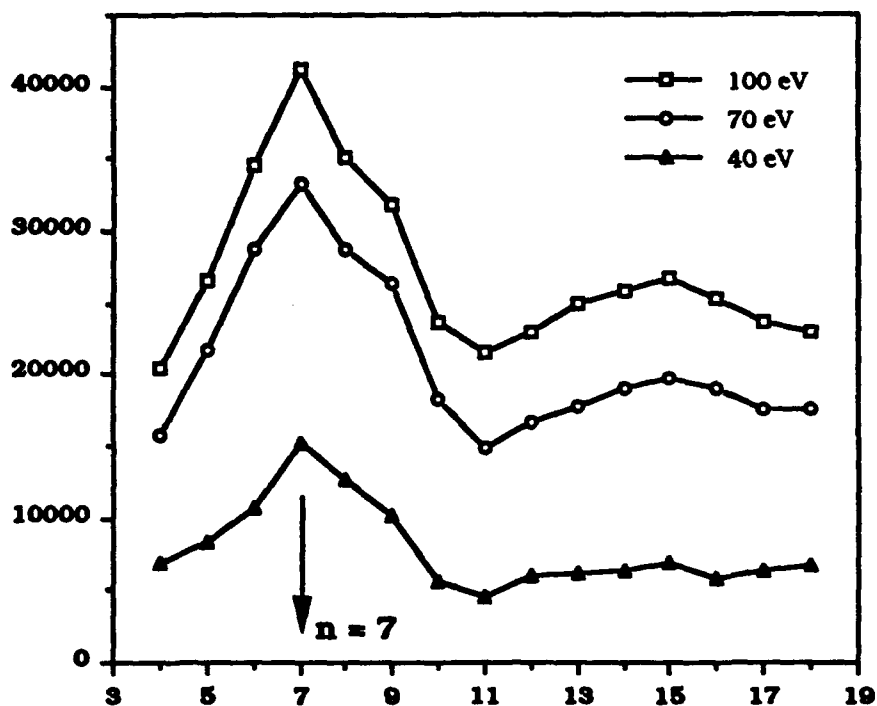


Figure 2. Comparison of the mass spectra of the  $\text{CH}_3\text{OCH}_3$  and  $\text{CH}_3\text{OH}$  systems. (GAPOL ET AL.)



Ion Intensity (arb. units)

### Electron Energy Dependence



### Nozzle Temperature Dependence

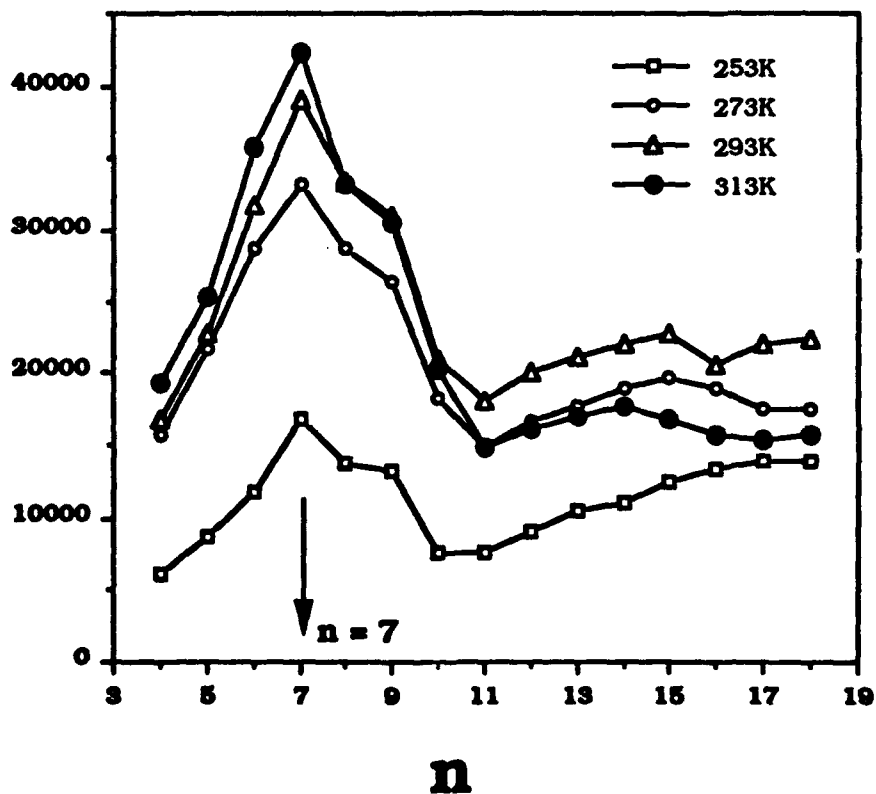


Figure 3, "Collision-Induced Ionization Cross-Sections of  $(\text{NH}_3)_n^+$

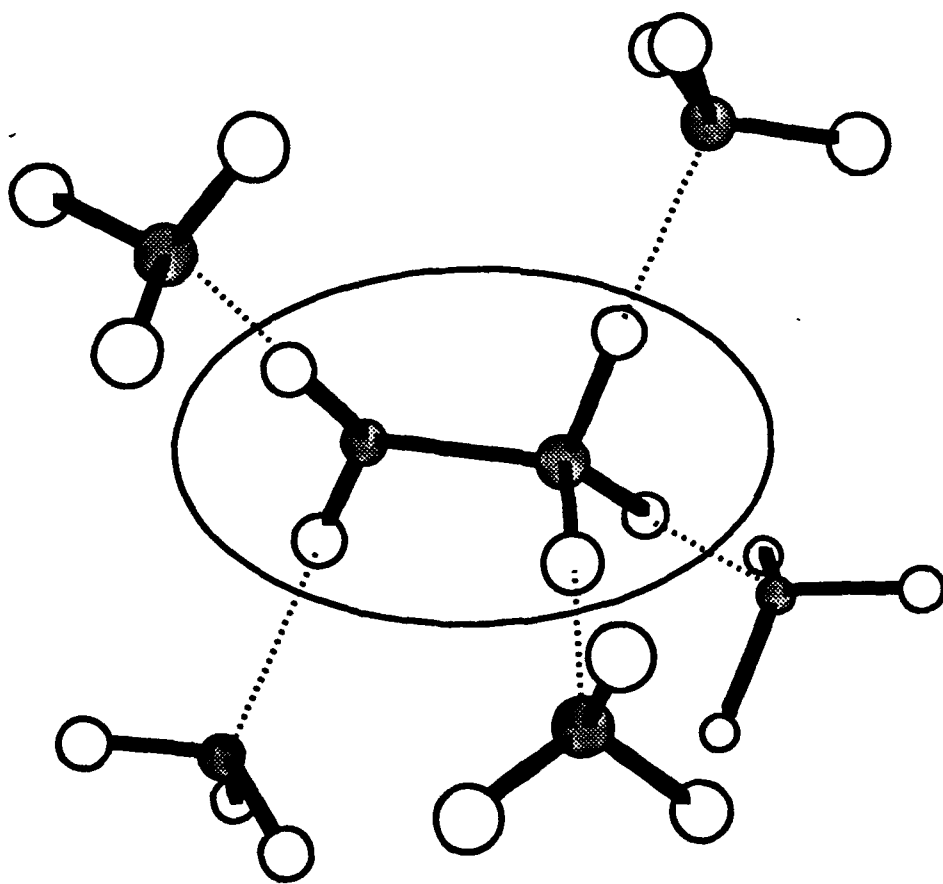
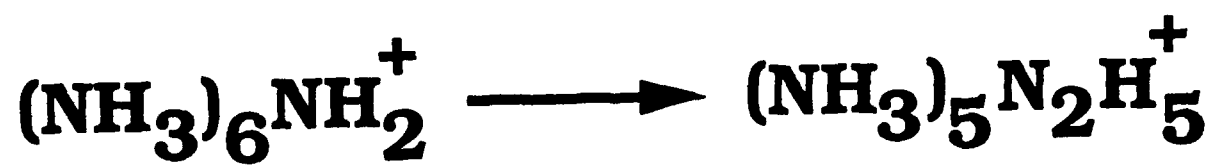


Figure 4. A computer-generated model of the transition state of the reaction.